

Optimization of synthesis conditions for *Calophyllum inophyllum* L.-loaded solid lipid nanoparticles[☆]

Sao Thi Ly^{1,2}, Anh Cam Ha^{1,2}, Ha Vu Le^{1,2}, Thanh-Thuy Thi Nguyen³, Viet Bao Nguyen⁴,
Ngoc-Lan Thi Nguyen⁵, Thuong-Nhan Phu Nguyen⁵, Thanh-Tra Thi Tran⁵ and Cang Huynh Mai^{5,*}

¹ Faculty of Chemical Engineering, Ho Chi Minh City University of Technology (HCMUT), 268 Ly Thuong Kiet Street, Dien Hong Ward, Ho Chi Minh City, Vietnam

² Vietnam National University Ho Chi Minh City, Linh Xuan Ward, Ho Chi Minh City, Vietnam

³ Department of Chemical Engineering and Processing, Nong Lam University, Thu Duc District, Ho Chi Minh City, Vietnam

⁴ Department of Chemical Engineering, Faculty of Chemical Engineering and Food Technology, Nong Lam University, Ho Chi Minh, Vietnam

⁵ Department of Natural Products, Faculty of Chemical Engineering and Food Technology, Nong Lam University, Thu Duc District, Ho Chi Minh City, Vietnam

Received 1 October 2025 – Accepted 29 January 2026

Abstract – Background: This study aimed to optimize the synthesis conditions for solid lipid nanoparticles (SLNs) loaded with *Calophyllum inophyllum* L. (tamanu) oil, a natural extract known for its anti-inflammatory, antimicrobial, and wound-healing properties. **Methods:** SLNs were prepared using a hot homogenization–ultrasonication–cold homogenization method, and various formulation parameters were systematically evaluated, including the type and concentration of solid lipids, hydrophilic–lipophilic balance (HLB) of surfactants, sonication power, and homogenization speeds. **Results:** Among the tested lipids, Naterol[®] SE produced stable SLNs and was selected for further optimization. Response Surface Methodology (RSM) with a Central Composite Design (CCD) was applied to model the effects of four key factors—HLB value, sonication power, hot homogenization speed, and cold homogenization speed—on particle size and polydispersity index (PDI). The optimized formulation achieved a mean particle size of 148.7 ± 1.39 nm and a PDI of 0.30, with spherical morphology confirmed by SEM and good physical stability under different storage conditions. **Objectives:** These findings demonstrate that the optimized tamanu oil-solid lipid nanoparticles (TO-SLNs) possess favorable physicochemical characteristics, offering strong potential as a topical nanocarrier system for skin repair and regeneration applications.

Keywords: Solid lipid nanoparticles (SLNs) / *Calophyllum inophyllum* L / Tamanu oil / Sonication power

Résumé – Optimisation des conditions de synthèse de nanoparticules lipidiques solides chargées en *Calophyllum inophyllum* L.. **Contexte :** Cette étude visait à optimiser les conditions de synthèse de nanoparticules lipidiques solides (NLS) chargées en huile de *Calophyllum inophyllum* L. (tamanu), un extrait naturel reconnu pour ses propriétés anti-inflammatoires, antimicrobiennes et cicatrisantes. **Méthodes :** Les NLS ont été préparées par une méthode combinant homogénéisation à chaud, ultrasonication et homogénéisation à froid. Différents paramètres de formulation ont été évalués de manière systématique, notamment le type et la concentration en lipides solides, l'équilibre hydrophile-lipophile (HLB) des tensioactifs, la puissance de sonication ainsi que les vitesses d'homogénéisation. **Résultats :** Parmi les lipides testés, le Naterol[®] SE a permis d'obtenir des NLS stables et a été retenu pour l'optimisation. Une méthodologie RSM (*Response Surface Methodology*) basée sur un plan composite central (*Central Composite Design*, CCD) a été appliquée afin de modéliser l'effet de quatre facteurs clés — la valeur du HLB, la puissance de sonication, la vitesse d'homogénéisation à chaud et la vitesse d'homogénéisation à froid — sur la taille des particules et l'indice de polydispersité (PDI). La formulation optimisée a permis d'obtenir une taille moyenne de particules de $148,7 \pm 1,39$ nm et un PDI de 0,30. La morphologie sphérique

[☆] Contribution to the Topical Issue: “Lipids and Cosmetics / Lipides et cosmétiques”.

*Corresponding author: maihuyhncang@hcmuaf.edu.vn

a été confirmée par microscopie électronique à balayage (MEB), et une bonne stabilité physique a été observée dans différentes conditions de stockage. **Objectifs** : Ces résultats montrent que les nanoparticules lipidiques solides à base d'huile de tamanu (TO-NLS) optimisées présentent des caractéristiques physico-chimiques favorables, offrant un fort potentiel en tant que système nanovecteur topique pour des applications de réparation et de régénération cutanées.

Mots-clés : Nanoparticules lipidiques solides (NLS) / *Calophyllum inophyllum* L / Huile de tamanu / Puissance de sonication

Highlights

- Naterol[®] SE produced stable solid lipid nanoparticles (SLNs) loaded with *Calophyllum inophyllum* L. (tamanu) oil.
- The optimized formulation achieved a mean particle size of 148.7 ± 1.39 nm and a PDI of 0.30, with spherical morphology confirmed by SEM.
- These nanoparticles (SLN-tamanu oil) were found to be physically stable under a range of storage conditions (refrigerated, room temperature, and elevated temperature), demonstrating their robustness for potential commercial use.

1 Introduction

Tamanu oil (TO), extracted from the nuts of *Calophyllum inophyllum* L., comes from an evergreen tree that flourishes in tropical coastal regions of Asia, Africa, and the Pacific Islands. The oil extraction process involves pressing the seeds to produce a rich, dark green oil known for its distinct nutty aroma. Studies have shown that tamanu oil possesses anti-inflammatory, antimicrobial, and wound-healing properties, making it a valuable asset in natural skincare and traditional medicine (Pribowo *et al.*, 2021). The composition of crude tamanu oil contains 71.5%–90.3% fat and 9.7%–28.5% resin. The fatty acid composition of tamanu oil includes palmitic acid ($16.5 \pm 1.59\%$), stearic acid ($30.2 \pm 4.36\%$), oleic acid ($23.6 \pm 4.77\%$), and linoleic acid ($25.5 \pm 3.87\%$). Minor components consist of palmitoleic acid ($0.26 \pm 0.11\%$), alpha-linolenic acid ($0.26 \pm 0.05\%$), arachidonic acid ($0.6 \pm 0.09\%$), gadoleic acid ($0.3 \pm 0.1\%$), dihomo-gamma-linolenic acid ($< 0.1\%$), behenic acid ($0.1 \pm 0.15\%$), and docosadienoic acid ($1.4 \pm 5.08\%$) (Raharivelomanana *et al.*, 2018). Tamanu oil harbors key bioactive constituents including 4-phenylcoumarin derivatives, calophyllolide, and inophyllolide compounds. Xanthones and coumarin derivatives have been shown to exert inhibitory effects on the proliferation of various cancer cell types, including those originating from the prostate, kidney, breast, larynx, lung, and colon, as well as central nervous system tumors, leukemia, and malignant melanoma (Hapsari *et al.*, 2023). Calophyllolide has been reported to possess strong anti-inflammatory properties, particularly when compared to hydrocortisone (10 mg), which was used as the positive control in formaldehyde induced arthritis models, showing an effectiveness from its efficient dose (ED) of 140mg/kg and its lethal dose (DL) of 2.5g/kg (Raharivelomanana *et al.*, 2018). Inophyllum C, E, and A have been reported to

exhibit both anticancer and anti-HIV activities. In contrast, inophyllum P and B demonstrate promising potential as HIV inhibitors (Hapsari *et al.*, 2023). Furthermore, tamanu oil has been recognized for its wound-healing capacity, antioxidant activity, antimicrobial effects, and ultraviolet (UV) absorption properties (Ferdosh, 2024; Raharivelomanana *et al.*, 2018).

Recent advancements in materials science and nanotechnology have enabled the precise fabrication of materials with particle sizes spanning from the micrometer to the nanometer scale. Nanoparticles with small size and very large surface area make them easily pass through biological cell membranes, are good drug delivery systems and interact quickly with biological systems in the body. However, nanomaterials with excellent biodegradability and biocompatibility are considered to be the best vehicles for drug delivery systems in biomedical applications (Duan *et al.*, 2020). Consequently, nanocarriers are being actively explored in the pharmaceutical and medical fields for applications such as biosensing, imaging, and targeted drug delivery. Nanoparticle-based drug carriers under research include dendrimers, metallic nanoparticles, and quantum dots that are either conjugated or coated with drug molecules on their surface, and lipid-based nano-carriers which include nanoemulsions, polymeric nanoparticles, niosomes, solid lipid nanoparticles (SLN), and liposomes (Mirchandani *et al.*, 2021). Among these diverse platforms, lipid-based systems are particularly attractive due to their inherent biocompatibility and use of physiologically safe components. Specifically, Solid Lipid Nanoparticles (SLNs) developed to synergistically combine the advantages of other systems, such as the stability of polymeric nanoparticles and the biocompatibility of liposomes and emulsions (Garud *et al.*, 2012; Mirchandani *et al.*, 2021). The solid matrix in SLNs also proposes to protect the loaded therapeutic molecules against the rough biological environment and also shield the other chemical degradations with maximum feasibility to alter the release profiles of the therapeutic molecule. Altogether, these proficiencies make the SLNs an exceptional carrier system (Sastri *et al.*, 2020). Therefore, solid lipid nanoparticles (SLNs) have attracted considerable global research interest due to their potential to achieve controlled and site-specific drug delivery, minimize toxicity, enhance bioavailability, and improve the overall pharmacokinetic performance of therapeutic agents (Badawi *et al.*, 2018; Mirchandani *et al.*, 2021). In a patent application from the early 1990s, Müller and Lucks were the first to describe SLNs and the production process (Viegas *et al.*, 2023). And since then, this term has been used more and more widely in research and many applications in several areas of life, such as pharmaceuticals, cosmetics and personal care, food and nutraceuticals. Solid lipid nanoparticles (SLNs) are the first generation of lipid-based

Table 1. Relationship between coded variables and factor levels.

Coded variables	Factor levels			
	A	B (%)	C (rpm)	D (rpm)
-2	9	40	8,000	8,000
-1	10	50	9,000	9,000
0	11	60	10,000	10,000
1	12	70	11,000	11,000
2	13	80	12,000	12,000

nanocarriers that are formulated from lipids, which are solid at body temperature and stabilized by emulsifiers (Ghasemiyeh and Mohammadi-Samani, 2018).

Although previous studies have highlighted the therapeutic potential of tamanu oil and SLNs, many of them relied on one-variable-at-a-time experimental designs, in which formulation or processing parameters were optimized individually without considering their interactions. In addition, key process variables such as surfactant HLB value, sonication energy, and homogenization conditions were often fixed or insufficiently explored, while stability evaluations were frequently limited to short-term observation under a single storage condition, resulting in inconsistent stability outcomes across studies (Mai *et al.*, 2019). To address this gap, the present study applies Response Surface Methodology (RSM) with Central Composite Design (CCD) to systematically optimize formulation parameters. This approach ensures robust particle size control, improved stability, and enhanced applicability in pharmaceutical and cosmeceutical fields.

2 Materials and methods

2.1 Materials

Calophyllum inophyllum refined oil (tamanu oil) was kindly gifted from Nong Lam University. The physicochemical properties of the refined tamanu oil are summarized in Table 1 (Supplementary Material), including viscosity (42.9 mPa·s), relative density (0.9102 ± 0.0001), acid value (0.112 ± 0.001 mg KOH/g sample), and saponification value (180.837 ± 2.355 mg KOH/g sample). Cetiol[®] SB 45 (the melting points: 42–46 °C) was purchased from BASF (Germany). Naterol[®] SE (the dropping point: 49–51 °C) and Naterol[®] 165 CN (the melting points: 55–59 °C) were purchased from CISME (Italy). IMWITOR[®] 900 K (the melting points: 54–66 °C) from IOI Oleo (Germany). Compritol[®] 888 CG ATO (the melting points: 70–75 °C) was purchased from Gattefossé (France). All other chemicals including Tween 80 from Evonik (Germany) and Span 80 from Croda (Singapore).

2.2 Preparation of Tamanu Oil-Load SLNs

In this study, solid lipid nanoparticles (SLNs) loaded with tamanu oil were prepared using the hot homogenization–sonication–cold homogenization method as described by Carlotti *et al.*, (2012). Briefly, tamanu oil and solid lipid were melted together above the lipid melting point from 5–10 °C

above their respective melting points and dispersed into a pre-heated aqueous surfactant solution followed by high-shear homogenization to form a coarse emulsion, probe sonication to reduce droplet size, and cold homogenization was performed at 0–5 °C to solidify the lipid matrix and obtain stable nanoparticles. To further optimize the formulation, several critical factors were systematically investigated. The effect of tamanu oil content (1.5–3.5% w/v) and total oil phase (6.5–8.5% m/v) was examined to determine their impact on particle size distribution. The hydrophilic–lipophilic balance (HLB) of Tween 80/Span 80 surfactant blends was varied across values of 9–13 to evaluate emulsification efficiency. Hot homogenization speed (8,000–12,000 rpm), sonication power (50–90% amplitude), and cold homogenization speed (8,000–12,000 rpm) were individually studied to understand their role in droplet disruption, particle stabilization, and final solidification. Collectively, these systematic experiments provided the basis for identifying optimal synthesis parameters to produce uniform, stable, and reproducible tamanu oil-loaded SLNs with desirable physicochemical properties.

2.3 Particle size analysis

The dynamic light scattering (DLS) technique was chosen for particle size as z-average diameter, PDI, and zeta potential of TO-SLNs evaluation by the using of Zetasizer Nano ZS (Malvern, United Kingdom). All analyses were performed in auto-measuring mode at 25 °C and the results were presented as the average value of triplicate samplings.

2.4 Stability of Tamanu Oil-Loaded SLNs

To assess the stability of the TO-SLNs, we conducted sensitivity experiments with different temperature (45 °C, room temperature and 10 °C) and UV light exposure. In parallel, a blank sample (SLN-FREE), a solid lipid suspension without tamanu oil, was prepared as a reference sample for a comparison of the stability of SLNs.

2.5 Optimization TO-loaded SLNs of synthetic procedure by RSM

The synthesis procedure of tamanu oil-loaded SLNs was statistically optimized using RSM-CCD design. Four independent variables were selected as critical formulation factors: HLB (A), sonication power (B), hot homogenization speed (C), and cold homogenization speed (D). A total of thirty

experimental runs were generated, including sixteen factorial points to assess linear and interaction effects, eight axial (star) points to capture quadratic responses and curvature, and six center points to estimate experimental error.

After identifying the central values of the key formulation variables, experimental regions were established for four independent factors: HLB value (A), sonication power (B), hot homogenization speed (C), and cold homogenization speed (D). The center points were set at HLB = 11, sonication power = 60%, hot homogenization = 10,000 rpm, and cold homogenization = 10,000 rpm, with survey ranges spanning from HLB 9–13, sonication 40–80%, and homogenization speeds 8,000–12,000 rpm. To ensure orthogonality and facilitate correlation analysis, all factor levels were encoded into dimensionless units, where the central point was assigned a value of 0, the lowest and highest levels were coded as -2 and $+2$, and intermediate values as -1 and $+1$. The relationship between actual and coded factor levels is summarized in [Table 1](#).

2.6 Statistical analysis

All experiments were performed in triplicate, and the data are presented as mean \pm standard deviation (SD). Statistical analyses were conducted using Design-Expert[®] software (version XX, Stat-Ease Inc., Minneapolis, MN, USA) for model fitting and response surface methodology (RSM). Analysis of variance (ANOVA) was applied to evaluate the significance of the regression models and individual terms. Differences were considered statistically significant at $p < 0.05$.

3 Results

The experiments in this study were conducted in two stages. First, preliminary single-factor tests were performed to examine the effects of lipid type, lipid concentration, HLB value, sonication power, and homogenization speeds. These results helped define suitable working ranges and select the most stable lipid system.

In the second stage, four key factors (HLB, sonication power, hot and cold homogenization speeds) were optimized simultaneously using RSM–CCD to determine the conditions that yield the smallest and most uniform SLNs.

Accordingly, the results are presented in two parts: (3.1) Preliminary experiments and factor screening, and (3.2) RSM–CCD optimization.

3.1 Preliminary experimental and factor screening results

3.1.1 Selection of suitable Solid Lipids for SLNs

To establish an appropriate foundation for the optimization study, an initial screening was conducted to identify the most suitable solid lipid for forming stable tamanu oil-loaded SLNs. In this stage, five different solid lipids were tested under identical processing conditions ([Tab. 2](#)). All SLNs were produced using a standardized process consisting of hot homogenization (10 minutes at 8,000 rpm), probe sonication (10 minutes at 80% power), and cold homogenization

Table 2. Z-average and PDI of SLNs formulated by different solid lipid.

Solid lipid	Z-average (nm)	PDI
Naterol [®] 165 CN	157.5	0.320
Naterol [®] SE	275.2	0.259
Imwitor [®] 900 K	332.0	0.518
Compritol [®] 888 CG ATO	886.3	1.000

(10 minutes at 8,000 rpm). All tested solid lipids were evaluated at the same concentration to ensure a fair comparison. The formulation consisted of 2.5% (w/w) solid lipid, 5% (w/w) tamanu oil, 3.6% (w/w) Tween 80, 1.4% (w/w) Span 80, and distilled water added to 100%. The tested lipids included Naterol[®] 165 CN, Naterol[®] SE, IMWITOR[®] 900 K, Compritol[®] 888 ATO. Cetiol[®] SB 45 was excluded from further analysis because it did not form a stable dispersion during preparation. This preliminary screening provided the basis for identifying the lipid system with the most favorable particle size and stability for subsequent optimization.

The SLNs prepared with Naterol[®] 165 CN exhibited the smallest average particle size of 157.5 nm with a PDI of 0.32, indicating a relatively narrow size distribution. Naterol[®] SE produced SLNs with a slightly larger average size of 275.2 nm but a lower PDI of 0.259, suggesting a more uniform particle population. Imwitor[®] 900 K and Compritol[®] 888 CG ATO resulted in significantly larger particles, measuring 322.0 nm (PDI = 0.518) and 886.3 nm (PDI = 1.000), respectively, with Compritol-based SLNs showing a very broad size distribution and poor uniformity. Despite the smaller particle size achieved with Naterol[®] 165 CN, this formulation demonstrated physical instability, as evidenced by sedimentation occurring within one week of storage. In contrast, SLNs formulated with Naterol[®] SE remained physically stable without sedimentation, making it the preferred lipid for further optimization. These findings are consistent with previous reports indicating that glycerol stearate-based lipids such as Naterol[®] SE provide better emulsification properties and improved compatibility with amphiphilic surfactants, leading to more uniform particle populations and reduced sedimentation ([Ghasemiyeh and Mohammadi-Samani, 2018](#); [Sastri *et al.*, 2020](#)).

3.1.2 Determining the effect of the solid lipid ratio factor

To further refine the SLN formulation, the next step was to evaluate how the ratio of solid lipid affects particle size and dispersion quality. After identifying Naterol[®] SE as the most stable lipid system in [Section 3.1.1](#), different proportions of solid lipid were investigated to determine the concentration range that supports efficient nanoparticle formation.

As demonstrated in [Figure 1](#), an increase in solid lipid concentration from 1.5% to 3.5% (w/v) resulted in a progressive increase in the Z-average diameter of the SLNs, from 152.58 nm to 356.25 nm. This clear upward trend suggests that higher lipid content contributes significantly to the formation of larger nanoparticles. Similar observations have been reported in earlier studies. Müller *et al.* demonstrated that an increase in lipid concentration beyond an

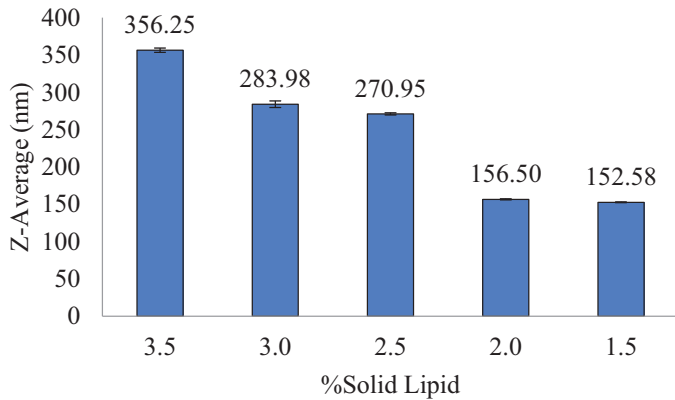


Fig. 1. Effect of solid lipid concentration on particle size (Z-Average).

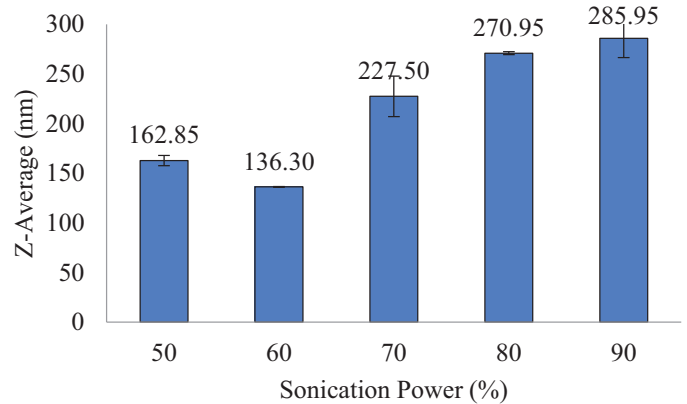


Fig. 3. Effect of sonication power on particle size.

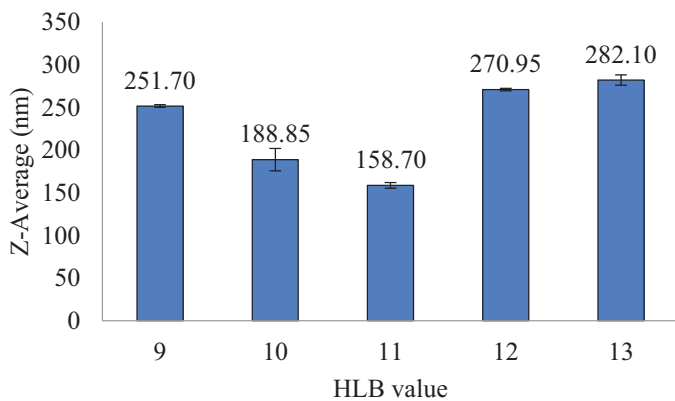


Fig. 2. Effect of HLB on particle size (Z-Average).

optimal range reduced emulsification efficiency, yielding particles with larger sizes and lower stability (Müller *et al.*, 2000). Mehnert and Mäder (2012) also emphasized that excess lipid can crystallize irregularly during cooling, further increasing heterogeneity and polydispersity.

3.1.3 Determining the effect of the HLB factor

To evaluate how surfactant polarity influences SLN formation, the effect of different HLB values in the surfactant blend was investigated. This experiment helps determine the appropriate HLB range required to obtain stable tamanu oil-loaded SLNs with small particle size.

The HLB (hydrophilic-lipophilic balance) of the surfactant blend significantly influenced the particle size of SLNs (Fig. 2). Among the tested HLB values (9 to 13), the smallest particle size (158.70 nm) was obtained at an HLB of 11. Deviations from this optimal HLB, either higher (13) or lower (9), resulted in larger particle sizes, with the highest value reaching 282.10 nm. These findings are consistent with recent studies that emphasize the importance of HLB optimization for lipid-based carriers, especially for achieving nanoscale dispersion and long-term stability (Ohadi *et al.*, 2020; Patel *et al.*, 2021).

3.1.4 Determining the effect of the sonication power factor

Sonication power plays an important role in reducing droplet size during emulsification, as ultrasonic cavitation helps break large droplets into smaller ones. Therefore, this section evaluates how different sonication power levels influence the particle size of tamanu oil-loaded SLNs.

The impact of sonication amplitude on the Z-average particle size of SLNs, as illustrated in Figure 3, reveals a notable U-shaped trend. Increasing the amplitude from 50% to 60% significantly reduced the particle size, reaching a minimum of 136.30 nm at 60% power. However, beyond this optimal point, further increases in sonication power (70%–90%) led to a counterintuitive rise in particle size, with the highest value recorded at 285.95 nm at 90% power. This U-shaped relationship can be explained by the balance between droplet disruption and destabilization (Shah *et al.*, 2024). Moderate sonication energy provides sufficient cavitation and shear to break down lipid droplets, while excessive energy generates local overheating and turbulent microenvironments that promote coalescence and destabilization of surfactant films (Gao and Meng, 2024).

3.1.5 Determining the effect of the hot homogenization speed factor

Hot homogenization speed plays an important role in reducing droplet size during the initial emulsification step. To evaluate its influence on SLN formation, different homogenization speeds were tested while keeping all other parameters constant.

As the homogenization speed increases from 8,000 rpm to 10,000 rpm, there is a noticeable decrease in particle size from 270.95 nm to 237.20 nm (Fig. 4). This trend can be attributed to the enhanced shear forces at higher speeds, which effectively break down lipid droplets into smaller particles. Higher processing temperatures during hot homogenization reduce the viscosity of the lipid phase, facilitating the formation of smaller particles (Mukherjee *et al.*, 2009). However, further increasing the homogenization speed to 11,000 rpm and 12,000 rpm resulted in a slight increase in particle size to 252.60 nm and 258.30 nm, respectively. The findings highlight that hot homogenization must be carefully controlled to

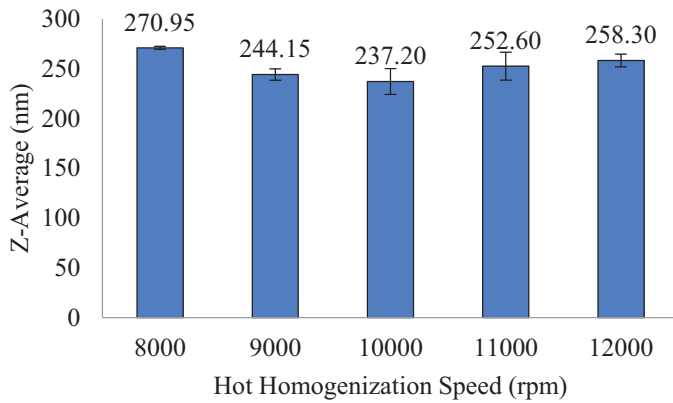


Fig. 4. Effect of hot homogenization speed on particle size.

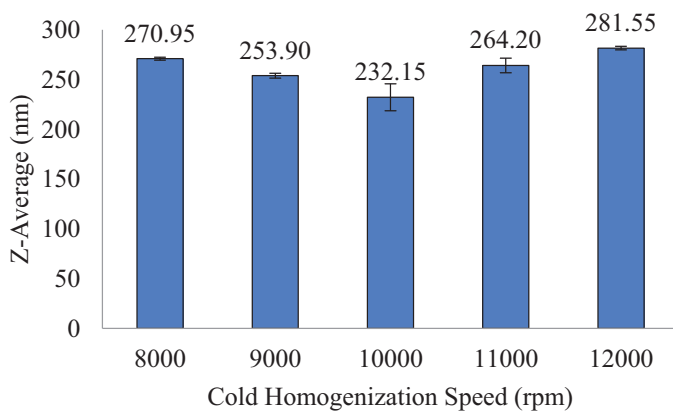


Fig. 5. Effect of cold homogenization speed on particle size.

maximize energy efficiency without exceeding the stability threshold of the emulsion (Håkansson, 2019).

3.1.6 Determining the effect of the cold homogenization speed factor

Cold homogenization speed factor investigates how different cold homogenization speeds influence the final size of SLNs.

The influence of cold homogenization speed on particle size is illustrated in Figure 5. The Z-average shows a distinct dependence on the homogenization speed. As the speed increases from 8,000 to 10,000 rpm, the average particle size decreases from 270.95 nm to 232.15 nm. However, further increasing the speed to 11,000 and 12,000 rpm leads to a paradoxical increase in particle size, with Z-averages of 264.20 nm and 281.55 nm, respectively. The increase at higher speeds can be attributed to excessive mechanical stress during lipid crystallization, which may interfere with surfactant adsorption or induce particle aggregation. Conversely, insufficient homogenization leads to incomplete dispersion (Gao and Meng, 2024; Khairnar *et al.*, 2022). Therefore, an intermediate cold homogenization speed (around 10,000 rpm) provides the best balance between mechanical mixing and structural stabilization, supporting efficient solidification of the lipid matrix.

Table 3. Summary of optimal conditions.

Factor	Level
HLB	11
Sonication power (%)	60
Hot homogenization speed (rpm)	10,000
Cold homogenization speed (rpm)	10,000

3.2 RSM–CCD optimization results

From the appropriate intervals in section 3.1, four major factors—HLB value, sonication power, hot homogenization speed, and cold homogenization speed—were simultaneously evaluated to determine their individual and interactive effects on particle size. Table 3 summarized the suitable parameters for producing SLN-loaded with tamanu oil.

3.2.1 Optimization of SLNs size

The independent variables studied were: HLB value, sonication power (%), hot homogenization speed (rpm), and cold homogenization speed (rpm). The responses measured included the Z-average particle size (Y_1 , in nm) and the polydispersity index (Y_2 , PDI), both critical for evaluating the quality and stability of the SLNs formulation (Tab. 4).

3.2.2 Overview of Z-average results

The Z-average values obtained from the 30 experimental runs were analyzed to assess how the combined formulation influenced particle size behavior across the CCD model.

Across the 30 runs, Z-average values ranged from 140.3 nm to 228.3 nm, while PDI ranged from 0.149 to 0.48 (Fig. S6). This wide distribution demonstrates that the formulation and process variables significantly influence both particle size and size distribution. Notably, the five replicated center point runs (Runs 25–30) with HLB = 11, sonication power = 60%, hot homogenization = 10,000 rpm, and cold homogenization = 10,000 rpm consistently yielded the smallest Z-average values (140.3–141.7 nm), with a mean around 141 nm, indicating high reproducibility and formulation robustness. The HLB value exerted a considerable influence on particle size. Under identical process conditions (Runs 17, 18, and 25–30), decreasing the HLB to 9 (Run 17) or increasing it to 13 (Run 18) led to much larger particle sizes—223.7 nm and 228.3 nm, respectively—compared to 141 nm at HLB 11. This confirms that optimal emulsification and stabilization occur when the HLB of the surfactant system is closely matched to the polarity of the lipid phase, with HLB 11 emerging as the optimal value (Miranda-Olvera *et al.*, 2025). The influence of sonication power followed a non-linear trend. At constant HLB = 11 and homogenization speeds, 60% sonication (Run 25: 141.2 nm) yielded the smallest particles. Both lower (40%, Run 19: 173.4 nm) and higher power (80%, Run 20: 174.6 nm) produced larger particles. This trend supports the hypothesis that low power provides insufficient droplet disruption, while excessive power may cause local

Table 4. Experimental design matrix and results for SLN-loaded *Calophyllum inophyllum* L. extract.

Std	Factors				Responses	
	HLB	Sonication power (%)	Hot homogenization speed (rpm)	Cold homogenization speed (rpm)	Z-average (nm)	PDI
1	10	50	9000	9000	191.6	0.333
2	12	50	9000	9000	147.0	0.254
3	10	70	9000	9000	204.7	0.329
4	12	70	9000	9000	187.3	0.149
5	10	50	11000	9000	166.2	0.355
6	12	50	11000	9000	143.0	0.242
7	10	70	11000	9000	179.1	0.421
8	12	70	11000	9000	144.1	0.446
9	10	50	9000	11000	178.3	0.440
10	12	50	9000	11000	158.2	0.413
11	10	70	9000	11000	172.9	0.434
12	12	70	9000	11000	236.9	0.271
13	10	50	11000	11000	154.3	0.432
14	12	50	11000	11000	171.3	0.272
15	10	70	11000	11000	162.8	0.480
16	12	70	11000	11000	209.2	0.228
17	9	60	10000	10000	245.4	0.331
18	13	60	10000	10000	207.0	0.166
19	11	40	10000	10000	147.0	0.305
20	11	80	10000	10000	179.7	0.301
21	11	60	8000	10000	144.9	0.308
22	11	60	12000	10000	142.2	0.397
23	11	60	10000	8000	129.2	0.323
24	11	60	10000	12000	159.0	0.356
25	11	60	10000	10000	141.2	0.312
26	11	60	10000	10000	141	0.308
27	11	60	10000	10000	145.4	0.311
28	11	60	10000	10000	140.3	0.306
29	11	60	10000	10000	139.4	0.302
30	11	60	10000	10000	141.7	0.283

overheating and bubble formation, disrupting surfactant stabilization and promoting coalescence.

Hot homogenization generally improved particle size reduction up to an optimal point. At fixed HLB and sonication settings (Runs 21, 25, and 22), increasing the hot homogenization speed from 8,000 rpm to 10,000 rpm reduced Z-average from 144.9 nm to 141.2 nm, while a further increase to 12,000 rpm led to a larger particle size of 150.8 nm. This suggests that 10,000 rpm is the optimal setting, beyond which shear forces may destabilize emulsified droplets. Cold homogenization speed also showed a complex influence. Comparing Runs 23 and 24 (8,000 rpm vs. 12,000 rpm) at fixed HLB and sonication, increasing cold homogenization speed increased particle size from 187.7 nm to 214.2 nm. Excessive mechanical stress during the lipid solidification phase may interfere with surfactant film formation or induce aggregation, suggesting that moderate cold homogenization is more favorable.

3.2.3 Further analysis of polydispersity index (PDI)

A detailed evaluation of the PDI was conducted to assess the uniformity of particle size distribution and its relevance to SLN stability.

PDI values ranged from 0.149 to 0.48 across 30 experimental runs (Fig. S7). The lowest PDI (0.149) was observed in Run 4, which combined HLB 12, sonication power of 70%, hot homogenization at 9,000 rpm, and cold homogenization at 9,000 rpm. Interestingly, this run also had a moderate particle size (187.3 nm), suggesting that a narrow size distribution can occur even when the average size is not minimized - highlighting that PDI and Z-average are related but not always directly proportional. The most consistent and favorable PDI values were observed in the five replicated center point runs (Runs 25–30), all with HLB = 11, sonication power = 60%, hot and cold homogenization = 10,000 rpm. These runs yielded PDIs ranging from 0.283 to 0.312, with an average of 0.305. While slightly above the strict 0.3 threshold, these values are still within an acceptable range for practical formulations and indicate good reproducibility and formulation stability. On the contrary, some runs showed significantly higher PDI values, exceeding 0.4 (Run 15 and Run 7). These results suggest that higher sonication powers (70–90%) and simultaneously high homogenization speeds may increase shear-induced droplet coalescence or result in poor surfactant film formation during emulsification and solidification. This leads to a broader size distribution and is

Table 5. Variance analysis results of the Y_{size} objective function.

Std. Dev.	9.48	R^2	0.9351
Mean	176.30	Adjusted R^2	0.8745
C.V.%	5.38	Predicted R^2	0.6263
		Adeq Precision	14.1113

reflected in higher PDI values. Interestingly, PDI values were not solely dependent on the average particle size (Run 13 and Run 18). This again highlights that a formulation can produce small particles but with broad size variation, depending on how uniformly the energy (sonication/homogenization) is distributed and how effectively the surfactants stabilize the system (Rehman *et al.*, 2024).

Overall, the results demonstrate that both formulation factors and processing conditions strongly influence PDI. Among the tested variables, HLB, sonication power, and cold homogenization speed appeared to have the most pronounced effects on particle uniformity. Moderate sonication (60%), balanced homogenization speeds (around 10,000 rpm), and an HLB of 11 consistently produced lower PDI, reinforcing their selection for optimal nanoparticle formulation.

3.2.4 Statistical analysis and model fitting

The statistical analysis indicates that the fitted model is statistically significant, with an F -value of 15.43 and a p -value less than 0.0001. This implies that the model effectively explains the variability in SLNs particle size, and the likelihood that such a strong model arises purely by random chance is extremely low. The resulting regression equation, in coded terms, is:

$$Y_{\text{size}} = 141.03 + 5.63A + 8.23AD + 20.72A^2 + 7.72B^2 + 14.46D^2 \quad (1)$$

In which:

- A-HLB
- B-Sonication Power (%)
- C-Hot homogenization speed (rpm)
- D-Cold homogenization speed (rpm)

In the statistical evaluation of model fit (Tab. 5), the quadratic regression model for SLNs particle size exhibits both high precision and strong explanatory power, yet reveals areas for further refinement. The coefficient of determination, $R^2 = 0.9351$, signifies that 93.51% of the total variability in SLNs size is captured by the six retained terms, while the adjusted $R^2 = 0.8745$ remains high after penalizing for model complexity, indicating that the majority of predictors contribute meaningfully rather than inflating fit artificially. In practice, this model can guide the initial optimization of HLB, sonication energy, and cold homogenization parameters, provided that follow-up experiments are performed to validate and, if necessary, refine the predicted optimum regions.

In order to evaluate the adequacy of the fitted quadratic regression model for SLNs particle size, a formal lack-of-fit test was conducted (Tab. 6). The model itself is highly

Table 6. Model fit analysis table using F and P values.

Polynomial model	Model		Lack of fit	
	F -value	P	F -value	P
Y_{size}	15.43	<0.0001	<0.0001	<0.0001

significant, with an overall F -value of 15.43 ($p < 0.0001$), confirming that the chosen factors and their quadratic terms explain a substantial portion of the observed variability.

3.2.5 Response surface models

Response surface models provide an overview of the dependence and interaction of the factors of HLB with sonication power, hot homogenization speed, and cold homogenization speed (Figs. 6 and 7).

3.2.6 Determination of optimal point

Based on the constructed quadratic model and numerical optimization tools, the optimal point for minimizing Z-average particle size was identified. The optimal conditions suggested by the model were displayed at Table 7. At these optimized parameters, the predicted Z-average (Y_1) of the SLNs was 143.28 nm, indicating a highly uniform and nanoscale particle size ideal for topical and pharmaceutical applications.

3.2.7 Evaluation of the properties of optimal SLNs

3.2.7.1 Size and PDI

The model predicted a Z-average of 143.28 nm. The experimental values and corresponding relative errors are shown in Table 8.

The experimental Z-average values ranged from 147.7 to 150.4 nm, with relative errors of 3.08% to 4.98% compared to the predicted model value of 143.28 nm. The average particle size across all three trials was 148.7 ± 1.39 nm, which closely aligns with the model prediction and confirms the practical reliability of the optimization approach. The polydispersity index (PDI) ranged between 0.291 and 0.309, indicating a narrow and consistent particle size distribution. Although slightly above the 0.3 threshold for strict monodispersity, these values still reflect high formulation uniformity suitable for pharmaceutical use. Comparable results have been reported in earlier studies on SLNs. Badawi *et al.* (2018) achieved mean particle sizes of 145–160 nm with PDI values around 0.28–0.32 for pomegranate extract-loaded SLNs, emphasizing the robustness of similar lipid-based nanocarriers in maintaining nanoscale dimensions with moderate monodispersity (Badawi *et al.*, 2018). Meanwhile, Zhao *et al.* (2022) formulated SLNs with mean size 113.0 ± 0.8 nm at PDI 0.177 ± 0.007 , demonstrating that smaller sizes with lower PDI are achievable depending on lipid/surfactant composition (Zhao *et al.*, 2022).

3.2.7.2 Zeta potential

The zeta potential values measured for the optimized SLNs formulation across three independent batches were -5.25 mV, -5.35 mV, and -5.64 mV, respectively (Tab. 9). These results

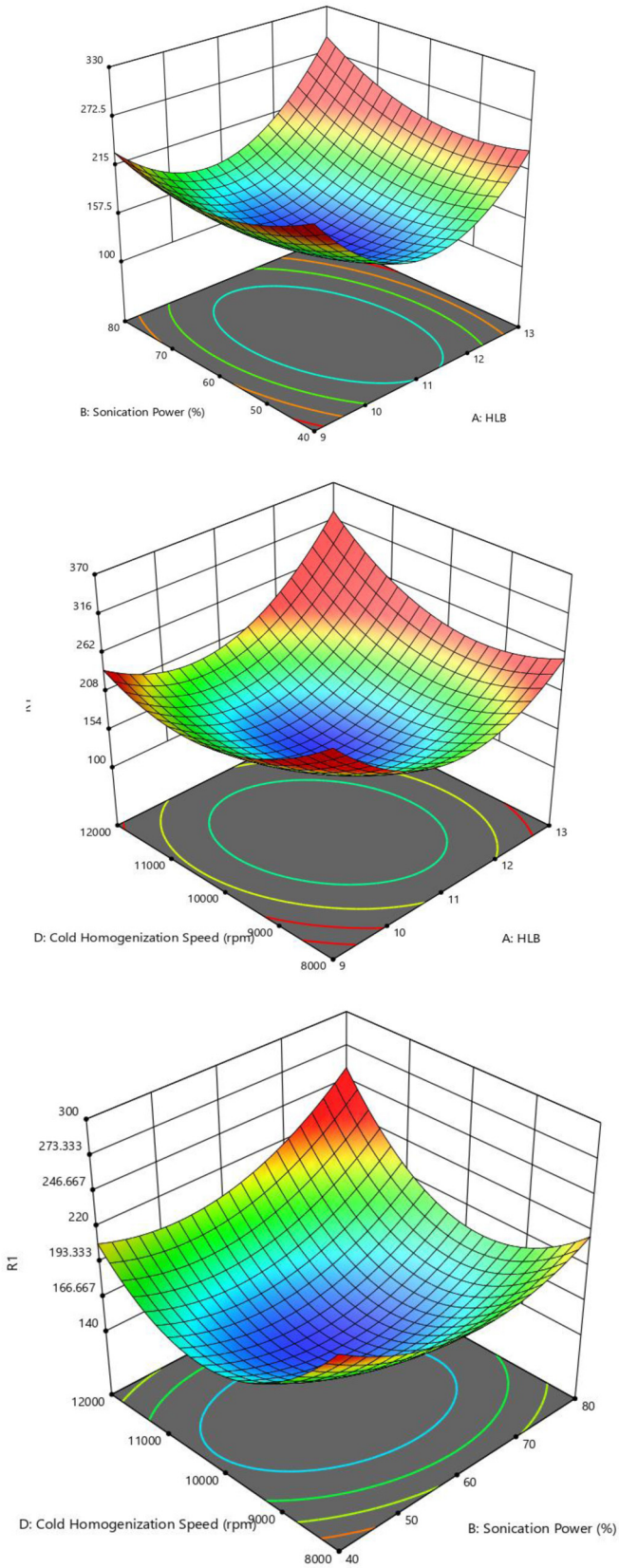


Fig. 6. 3D Response surface of formulation factors on SLNs size.

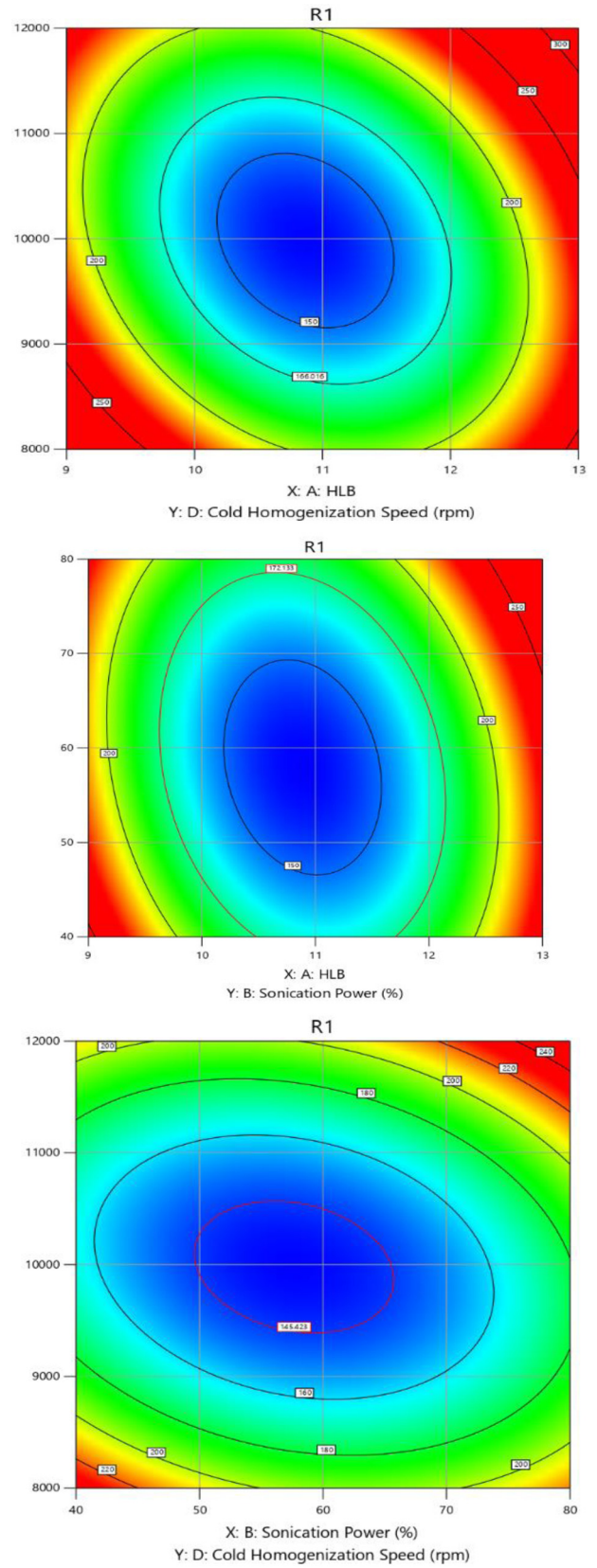


Fig. 7. Contour plots of formulation factors on SLNs size.

Table 7. Optimization conditions for Z-average.

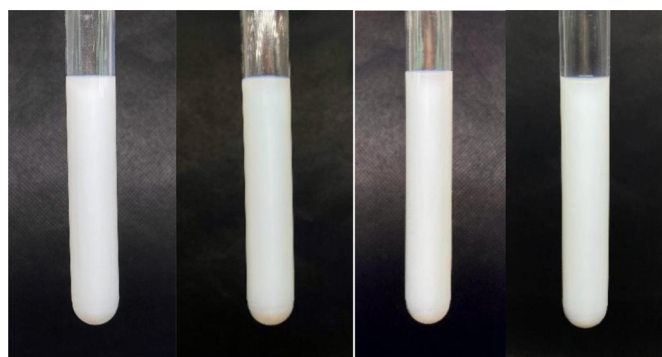
Factors	Level	Predicted Z-average (nm)
HLB	10.8	143.28
Sonication power (%)	59	
Hot homogenization speed (rpm)	10,500	
Cold homogenization speed (rpm)	10,000	

Table 8. Experimental vs. predicted Z-average.

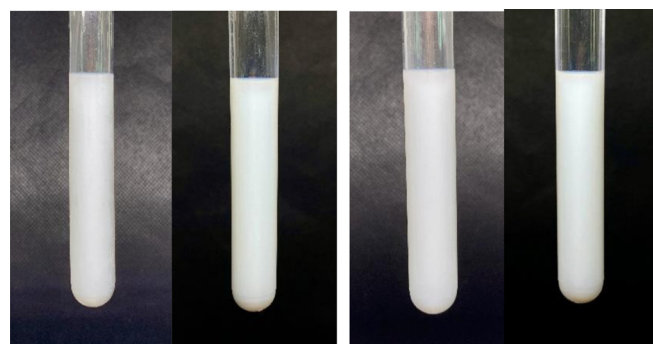
Trial	Z-average (nm)	PDI	Predicted Z-average (nm)	Relative error (%)
1	148.1	0.291	143.28	3.36
2	147.7	0.296		3.08
3	150.4	0.309		4.98

Table 9. Zeta potential of optimal SLNs.

Trial	Zeta potential (mV)	Average zeta potential (mV)
1	-5.25	-5.41 ± 0.20
2	-5.35	
3	-5.64	

**Fig. 8.** Optimal samples 1 (left) and 2 (right) under refrigeration conditions (0–10 °C) over 2 weeks.

indicate that the nanoparticles possess a slightly negative surface charge, which is primarily attributed to the weak ionization of the lipid matrix and any residual charges from the encapsulated tamanu oil or surfactants (Nair *et al.*, 2022). Similar findings were noted by Beloqui *et al.* (2016), who observed that SLN systems formulated with non-ionic surfactants generally display low negative zeta potentials, typically in the range of -5 to -15 mV. In such cases, the long-term stability of the dispersion is maintained predominantly through steric effects provided by the surfactant layer rather than by strong electrostatic repulsion (Beloqui *et al.*, 2016).

**Fig. 9.** Optimal samples 1 (left) and 2 (right) under room conditions (30–33 °C) over 2 weeks.**Fig. 10.** Optimal samples 1 (left) and 2 (right) under room conditions (45–50 °C) over 2 weeks.

3.2.7.3 Stability of Tamanu Oil-Loaded SLNs

Temperature plays a crucial role in the behavior of solid lipid nanoparticles, as short-term exposure to elevated temperatures during transportation, packaging, storage, or sterilization can significantly affect their physicochemical stability (Sun *et al.*, 2020).

The stability of the optimized sample was evaluated by monitoring for any signs of phase separation under three different storage conditions: refrigeration (0–10 °C), room temperature (30–33 °C), and incubator conditions (45 °C). Evidence of phase separation under these storage conditions is illustrated in Figures 8–10.

Figures 8–10 illustrate the effect of storage conditions on SLNs stability. Under refrigeration (0–10 °C), both samples remained intact without visible separation, confirming good stability at low temperature. At room temperature (30–33 °C), the dispersions also showed no obvious creaming or sedimentation over two weeks, indicating that steric stabilization by surfactants was sufficient for short-term storage. In contrast, incubation at 45–50 °C led to partial phase separation, suggesting that thermal stress accelerates lipid polymorphic transitions and weakens surfactant adsorption (Cholakova *et al.*, 2020). Our results are consistent with the observations of Ball *et al.* (2017), who reported that keeping SLNs under refrigeration delays lipid recrystallization processes, thereby improving their

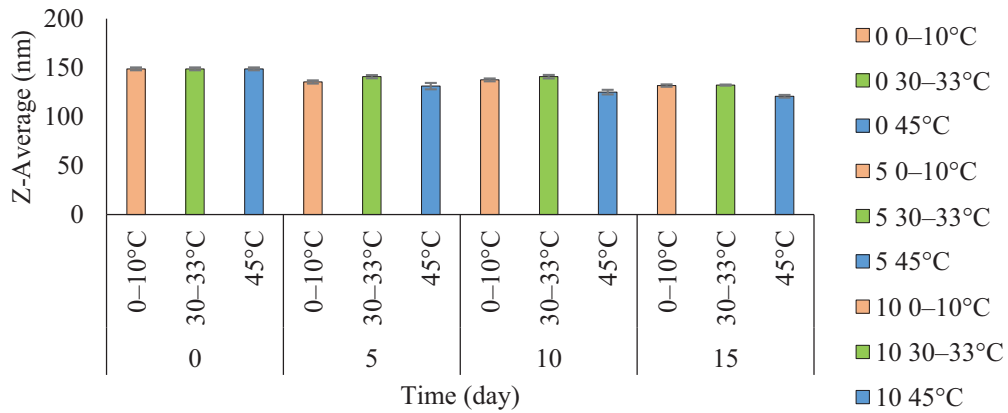


Fig. 11. Z-average particle size of tamanu oil-loaded SLNs during storage at different temperatures.

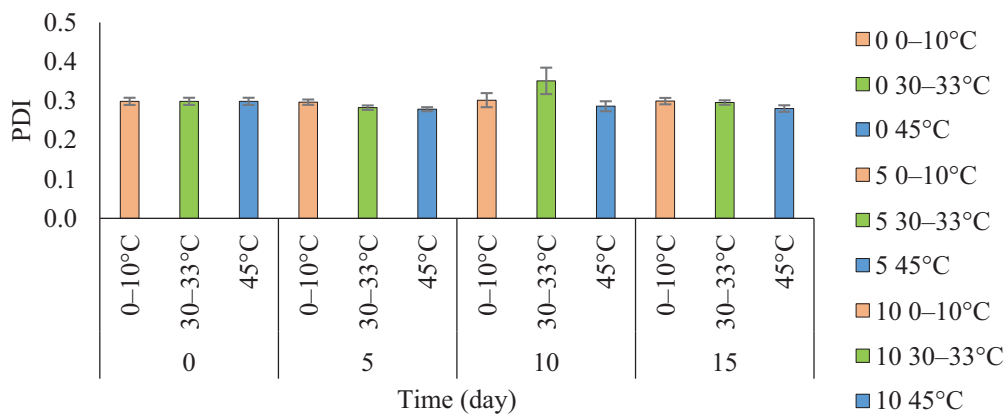


Fig. 12. PDI values of tamanu oil-containing SLNs during storage at different temperatures.

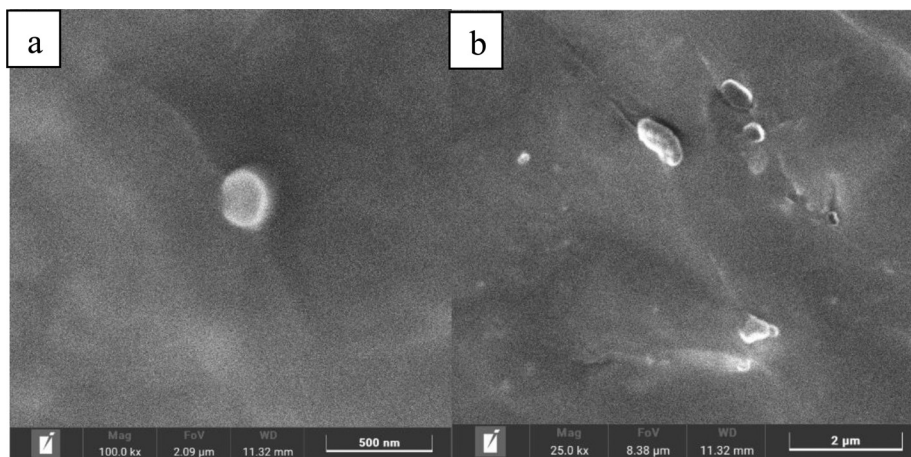


Fig. 13. SEM images of the *Calophyllum inophyllum* L.-loaded SLNs. *Note: Scale bar: 500 nm (a), 2 μ m (b).

stability relative to samples stored at room temperature or higher (Ball *et al.*, 2017).

The particle size and polydispersity index (PDI) of tamanu oil-loaded SLNs were monitored over 15 days under three storage conditions (0–10 °C, 30–33 °C, and 45 °C) (Fig. 11). Overall, the SLNs exhibited good size stability during the storage period, with Z-average values remaining within a narrow range of approximately 120–150 nm.

At 0–10 °C and 30–33 °C, only minor fluctuations in particle size and PDI were observed (Fig. 12), indicating that the SLN system remained physically stable without noticeable aggregation or phase separation. In contrast, samples stored at 45 °C showed a gradual decrease in Z-average size and a slight increase in PDI, suggesting partial destabilization of the lipid matrix at elevated temperature.

Nevertheless, the PDI values remained below 0.35 throughout the study, demonstrating an acceptable size distribution and confirming that the tamanu oil-loaded SLNs maintain satisfactory short-term stability under refrigerated and ambient storage conditions.

Overall, these results are consistent with previous studies and confirm that the SLN system exhibits satisfactory stability under recommended storage conditions (Mai *et al.*, 2019).

3.2.7.4 SEM (scanning electron microscope)

The SEM image taken at 100000 × magnification (Fig. 13a) shows a solid lipid nanoparticle exhibiting near-spherical morphology with smooth surface textures. The diameter of this particle was estimated in the range between 170 and 175 nm. The SEM image at 25000× magnification (Fig. 13b) provides an overview of a larger field containing SLNs. This image reveals a population of solid lipid nanoparticles exhibiting predominantly small particle sizes, with generally spherical morphology and relatively smooth surfaces. While a few larger particles are visible in the field, they might be above the submicron scale. Some of these larger structures show signs of morphological deformation, such as flattened edges, irregular outlines, or partial collapse, which could be attributed to mechanical stress during drying, electron beam interaction, or intrinsic instability of oversized lipid particles. On the other hand, the majority of observed structures appear significantly smaller, with estimated sizes ranging from approximately 150 to 170 nm. In summary, SEM analysis of the sample consistently revealed a predominant population of small, well-dispersed nanoparticles with measured sizes ranging from approximately 150 to 175 nm. These values align closely with the Z-average diameter of 150.4 nm obtained from dynamic light scattering (DLS), suggesting that the technique captures a convergent size profile centered within the low nanometric range. The spherical morphology and smooth surface observed under SEM further support the stability findings in Section 3.8.3. Such uniform particle geometry reduces interfacial stress and minimizes aggregation, which may explain why the formulation remained macroscopically stable under refrigeration and ambient storage conditions (Nguyen VH, 2022).

These morphological characteristics are typical for solid lipid nanoparticles stabilized by non-ionic surfactants. Similar spherical profiles were documented by Beloqui *et al.* (2017), who emphasized that uniform surface texture enhances dispersion stability and reduces aggregation risk (Beloqui *et al.*, 2017). Likewise, Alloush and Demiralp (2025) observed that spherical SLNs provide improved drug loading efficiency and controlled release, compared with irregular morphologies prone to fusion and sedimentation (Alloush and Demiralp, 2025).

4 Conclusions

Formulations of TO-SLNs were optimized using a central composite design (CCD) which was successfully implemented to statistically optimize the formulation variables. The effects of four critical formulation variables - HLB value, sonication power, hot homogenization speed, and cold homogenization speed - were systematically evaluated with respect to two key response

parameters: Z-average particle size and polydispersity index (PDI). Among several lipid candidates, Naterol[®] SE was selected as the optimal solid lipid due to its favorable emulsification behavior, stability, and compatibility with the active compound. The optimized SLNs formulation achieved a small and consistent particle size of approximately 148 nm and a PDI of ~ 0.30, values that are highly desirable for dermal applications. These nanoparticles were found to be physically stable under a range of storage conditions (refrigerated, room temperature, and elevated temperature), demonstrating their robustness for potential commercial use. The optimized formulation demonstrates excellent physicochemical characteristics, potential for enhanced skin penetration, and suitability for topical use.

Furthermore, we propose the optimized TO-SLNs formula as the formula of choice for further investigations of TO as a promising wound healing applications, including entrapment efficiency evaluation and bioactivity confirmation, the SLN-based system holds significant promise for clinical and cosmeceutical applications targeting skin repair and regeneration.

Acknowledgments

This study was supported by Nong Lam University, Ho Chi Minh City, Vietnam.

Funding

This study was funded by the Ministry of Education and Training of Vietnam with the topic "Tinh chế dầu mù u (*Calophyllum inophyllum* L.) và tạo hạt nano chất béo rắn (solid lipid nanoparticles, SLN) cha da^u mù u (SLN-da^u mù u)- ứng dụng tạo màng PVA/Pectin)", code: B2025-NLS-03.

Conflicts of interest

The authors have no conflicts of interest to declare that are relevant to the content of this article.

Author contribution statement

Conceptualization: Sao Thi Ly, Anh Cam Ha
 Data curation: Ha Vu Le, Thanh-Thuy Thi Nguyen
 Investigation, Methodology: Viet Bao Nguyen, Ngoc-Lan Thi Nguyen
 Methodology: Thanh-Tra Thi Tran
 Writing – Original Draft Preparation: Sao Thi Ly, Thuong-Nhan Phu Nguyen
 Supervision: Cang Huynh Mai

Supplementary material

- Figure S1.** Effect of solid lipid concentration on PDI.
- Figure S2.** Effect of HLB on PDI.
- Figure S3.** Effect of sonication power on PDI.
- Figure S4.** Effect of hot homogenization speed on PDI.
- Figure S5.** Effect of cold homogenization speed on PDI.
- Figure S6.** Overview of Z-Average results.

Figure S7. Overview of PDI results.

Table S1. The physico-chemical properties of Tamanu oil.

Table S2. Fatty acid composition of Tamanu oil.

The Supplementary Material is available at <http://www.ocl-journal.org/10.1051/ocl/2026004/olm>.

References

- Alloush T, Demiralp B. 2025. A review of formulation strategies for cyclodextrin-enhanced solid lipid nanoparticles (SLNs) and nanostructured lipid carriers (NLCs). *Int J Mol Sci* 26(13): 6509. <https://doi.org/10.3390/ijms26136509>.
- Badawi NM, Teaima MH, El-Say KM, Attia DA, El-Nabarawi MA, Elmazar MM. 2018. Pomegranate extract-loaded solid lipid nanoparticles: design, optimization, and *in vitro* cytotoxicity study. *Int J Nanomed* 1313–1326. <https://doi.org/10.2147/IJN.S154033>.
- Ball RL, Bajaj P, Whitehead KA. 2017. Achieving long-term stability of lipid nanoparticles: examining the effect of pH, temperature, and lyophilization. *Int J Nanomed* 305–315. <https://doi.org/10.2147/IJN.S123062>.
- Beloqui A, del Pozo-Rodríguez A, Isla A, Rodríguez-Gascón A, Solinís MÁ. 2017. Nanostructured lipid carriers as oral delivery systems for poorly soluble drugs. *J Drug Deliv Sci Technol* 42: 144–154. <https://doi.org/10.1016/j.jddst.2017.06.013>.
- Beloqui A, Solinís MÁ, Rodríguez-Gascón A, Almeida AJ, Prévot V. 2016. Nanostructured lipid carriers: promising drug delivery systems for future clinics. *Nanomed: Nanotechnol Biol Med* 12 (1): 143–161. <https://doi.org/10.1016/j.jddst.2017.06.013>.
- Carlotti ME, Sapino S, Ugazio E, Gallarate M, Morel S. 2012. Resveratrol in solid lipid nanoparticles. *J Dispers Sci Technol* 33 (4): 465–471. <https://doi.org/10.1080/01932691.2010.548274>.
- Cholakova D, Glushkova D, Tcholakova S, Denkov N. 2020. Nanopore and nanoparticle formation with lipids undergoing polymorphic phase transitions. *ACS Nano* 14(7): 8594–8604. <https://doi.org/10.1021/acsnano.0c02946>.
- Duan Y, Dhar A, Patel C, *et al.* 2020. A brief review on solid lipid nanoparticles: Part and parcel of contemporary drug delivery systems. *RSC Adv* 10(45): 26777–26791. <https://doi.org/10.1039/D0RA03491F>.
- Ferdosh S. 2024. The extraction of bioactive agents from *Calophyllum inophyllum* L., and their pharmacological properties. *Sci Pharm* 92(1): 6. <https://doi.org/10.3390/sci-pharm92010006>.
- Gao Y, Meng Z. 2024. Crystallization of lipids and lipid emulsions treated by power ultrasound: a review. *Crit Rev Food Sci Nutr* 64 (7): 1882–1893. <https://doi.org/10.1080/10408398.2022.2119365>.
- Garud A, Singh D, Garud N. 2012. Solid lipid nanoparticles (SLN): method, characterization and applications. *Int Curr Pharm J* 1 (11): 384–393. <https://doi.org/10.3329/icpj.v1i11.12065>.
- Ghasemiyeh P, Mohammadi-Samani S. 2018. Solid lipid nanoparticles and nanostructured lipid carriers as novel drug delivery systems: applications, advantages and disadvantages. *Res Pharm Sci* 13(4): 288–303. <https://doi.org/10.4103/1735-5362.235156>.
- Håkansson A. 2019. Emulsion formation by homogenization: current understanding and future perspectives. *Annu Rev Food Sci Technol* 10(1): 239–258. <https://doi.org/10.1146/annurev-food-032818-121501>.
- Hapsari S, Jadid N, Aparamarta HW, Gunawan S. 2023. Impact of solvent type, solvent-water concentration, and number of stages on the extraction of coumarin mixture from tamanu (*Calophyllum inophyllum*) oil and its antioxidant activity. *Arab J Chem* 16(2): 104449. <https://doi.org/10.1016/j.arabjc.2022.104449>.
- Khairnar SV, Pagare P, Thakre A, *et al.* 2022. Review on the scale-up methods for the preparation of solid lipid nanoparticles. *Pharmaceutics* 14(9): 1886. <https://doi.org/10.3390/pharmaceutics14091886>.
- Mai HC, Nguyen TSV, Le THN, Nguyen DC, Bach LG. 2019. Evaluation of conditions affecting properties of gac (*Momordica cochinchinensis* Spreng) oil-loaded solid lipid nanoparticles (SLNs) synthesized using high-speed homogenization process. *Processes* 7(2): 90. <https://doi.org/10.3390/pr7020090>.
- Mehnert W, Mäder K. 2012. Solid lipid nanoparticles: production, characterization and applications. *Adv Drug Deliv Rev* 64: 83–101. <https://doi.org/10.1016/j.addr.2012.09.021>.
- Miranda-Olvera AD, Domínguez-Esquivel J-M, Martínez J. 2025. Hydrophilic–Lipophilic Balance (HLB) correlation method for the selection of ionic liquid surfactant modifiers of the viscosity and emulsion stability of heavy oils. *Langmuir* 41(13): 8753–8765. <https://doi.org/10.1021/acs.langmuir.4c05309>.
- Mirchandani Y, Patravale VB, S B. 2021. Solid lipid nanoparticles for hydrophilic drugs. *J Control Release* 335: 457–464. <https://doi.org/10.1016/j.jconrel.2021.05.032>.
- Mukherjee S, Ray S, Thakur R. 2009. Solid lipid nanoparticles: a modern formulation approach in drug delivery system. *Indian J Pharm Sci* 71(4): 349. <https://doi.org/10.4103/0250-474X.57282>.
- Müller RH, Mäder K, Gohla S. 2000. Solid lipid nanoparticles (SLN) for controlled drug delivery—a review of the state of the art. *Eur J Pharm Biopharm* 50(1): 161–177. [https://doi.org/10.1016/S0939-6411\(00\)00087-4](https://doi.org/10.1016/S0939-6411(00)00087-4).
- Nair A, Mallya R, Suvarna V, Khan TA, Momin M, Omri A. 2022. Nanoparticles—Attractive carriers of antimicrobial essential oils. *Antibiotics* 11(1): 108. <https://doi.org/10.3390/antibiotics11010108>.
- Nguyen VH, T V, Van TV, Dao HA, Lee B-J. 2022. Nanostructured lipid carriers and their potential applications for versatile drug delivery via oral administration. *OpenNano* 8: 100064. <https://doi.org/10.1016/j.onano.2022.100064>.
- Ohadi M, Shahrahan A, Dehghannoudeh N, Eslaminejad T, Banat IM, Dehghannoudeh G. 2020. Potential use of microbial surfactant in microemulsion drug delivery system: a systematic review. *Drug Des Devel Therapy* 541–550. <https://doi.org/10.2147/DDDT.S232325>.
- Patel D, Patel B, Thakkar H. 2021. Lipid based nanocarriers: promising drug delivery system for topical application. *Eur J Lipid Sci Technol* 123(5): 2000264. <https://doi.org/10.1002/ejlt.202000264>.
- Pribovo A, Girish J, Gustiananda M, Nandhira RG, Hartrianti P. 2021. Potential of Tamanu (*Calophyllum inophyllum*) oil for atopic dermatitis treatment. *Evidence-Based Complement Alternat Med* 2021(1): 6332867. <https://doi.org/10.1155/2021/6332867>.
- Raharivelomanana P, Ansel J-L, Lupo E, *et al.* 2018. Tamanu oil and skin active properties: from traditional to modern cosmetic uses. *Oléagineux, Corps Gras, Lipides* 5(5): D504. <https://doi.org/10.1051/ocl/2018048>.
- Rehman M, Tahir N, Sohail MF, *et al.* 2024. Lipid-based nanoformulations for drug delivery: an ongoing perspective. *Pharmaceutics* 16(11): 1376. <https://doi.org/10.3390/pharmaceutics16111376>.

- Sastri KT, Radha GV, Pidikiti S, Vajjhala P. 2020. Solid lipid nanoparticles: preparation techniques, their characterization, and an update on recent studies. *J Appl Pharm Sci* 10(6): 126–141. <https://doi.org/10.7324/JAPS.2020.10617>.
- Shah S, Madhu H, Soniwala M, *et al.* 2024. Lipid-based nanoparticles. *Nanocarrier Vaccines: Biopharmaceutics-Based Fast Track Development*, 241–273. <https://doi.org/10.1002/9781394175482.ch7>.
- Sun X, Pan C, Ying Z, *et al.* 2020. Stabilization of zein nanoparticles with k-carrageenan and tween 80 for encapsulation of curcumin. *Int J Biol Macromol* 146: 549–559. <https://doi.org/10.1016/j.ijbiomac.2020.01.053>.
- Viegas C, Patrício AB, Prata JM, Nadhman A, Chintamaneni PK, Fonte P. 2023. Solid lipid nanoparticles vs. nanostructured lipid carriers: a comparative review. *Pharmaceutics* 15(6): 1593. <https://doi.org/10.3390/pharmaceutics15061593>.
- Zhao W, Zeng M, Li K, *et al.* 2022. Solid lipid nanoparticle as an effective drug delivery system of a novel curcumin derivative: formulation, release *in vitro* and pharmacokinetics *in vivo*. *Pharm Biol* 60(1): 2300–2307. <https://doi.org/10.1080/13880209.2022.2136205>.

Cite this article as: Thi Ly S, Phu Thuong Nhan Nguyen, Anh Cam Ha, Ha Vu Le, Thanh-Thuy Thi Nguyen, Viet Bao Nguyen, Ngoc-Lan Thi Nguyen, Thanh-Tra Thi Tran, Cang Huynh Mai. 2026. Optimization of synthesis conditions for *Calophyllum inophyllum* L.-loaded solid lipid nanoparticles. *OCL* 33: 14. <https://doi.org/10.1051/ocl/2026004>